Aquatic Toxicology 238 (2021) 105914

Contents lists available at ScienceDirect

Aquatic Toxicology

journal homepage: www.elsevier.com/locate/aqtox

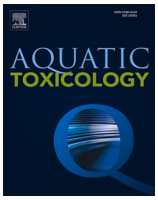

Polycyclic aromatic hydrocarbons modulate the activity of Atlantic cod (*Gadus morhua*) vitamin D receptor paralogs *in vitro*

Siri Øfsthus Goksøyr [a], Jed Goldstone [b], Roger Lille-Langøy [a], Erik-Jan Lock [a,c], Pål A. Olsvik [c,d], Anders Goksøyr [a], Odd André Karlsen [a,*]

[a] Department of Biological Sciences, University of Bergen, Norway
[b] Woods Hole Oceanographic Institution, Woods Hole, MA, USA
[c] Institute of Marine Research, Bergen, Norway
[d] Faculty of Biosciences and Aquaculture, Nord University, Bodø, Norway

ARTICLE INFO

Keywords:
Environmental toxicology
Antagonism
PAH
Calcitriol
Nuclear receptor
Potentiation

ABSTRACT

Vitamin D receptor (VDR) mediates the biological function of the steroid hormone calcitriol, which is the metabolically active version of vitamin D. Calcitriol is important for a wide array of physiological functions, including calcium and phosphate homeostasis. In contrast to mammals, which harbor one VDR encoding gene, teleosts possess two orthologous *vdr* genes encoding Vdr alpha (Vdra) and Vdr beta (Vdrb). Genome mining identified the *vdra* and *vdrb* paralogs in the Atlantic cod (*Gadus morhua*) genome, which were further characterized regarding their phylogeny, tissue-specific expression, and transactivational properties induced by calcitriol. In addition, a selected set of polycyclic aromatic hydrocarbons (PAHs), including naphthalene, phenanthrene, fluorene, pyrene, chrysene, benzo[a]pyrene (BaP), and 7-methylbenzo[a]pyrene, were assessed for their ability to modulate the transcriptional activity of gmVdra and gmVdrb *in vitro*. Both gmVdra and gmVdrb were activated by calcitriol with similar potencies, but gmVdra produced significantly higher maximal fold activation. Notably, none of the tested PAHs showed agonistic properties towards the Atlantic cod Vdrs. However, binary exposures of calcitriol together with phenanthrene, fluorene, or pyrene, antagonized the activation of gmVdra, while chrysene and BaP significantly potentiated the calcitriol-mediated activity of both receptors. Homology modeling, solvent mapping, and docking analyses complemented the experimental data, and revealed a putative secondary binding site in addition to the canonical ligand-binding pocket (LBP). Calcitriol was predicted to interact with both binding sites, whereas PAHs docked primarily to the LBP. Importantly, our *in vitro* data suggest that PAHs can interact with the paralogous gmVdrs and interfere with their transcriptional activities, and thus potentially modulate the vitamin D signaling pathway and contribute to adverse effects of crude oil and PAH exposures on cardiac development and bone deformities in fish.

1. Introduction

The vitamin D receptor (VDR, NR1I1) is a ligand-activated nuclear receptor transcription factor that mediates the biological function of the steroid hormone 1,25-dihydroxyvitamin D_3 ($1,25(OH)_2D_3$ or calcitriol), the metabolically active form of vitamin D (Reschly and Krasowski, 2006). In addition to some bile acids, such as lithocholic acid (LCA) and LCA derivatives, calcitriol is the only known endogenous agonist of VDR (Adachi et al., 2005, Adachi et al., 2004, Makishima et al., 2002, Krasowski et al., 2011a). Vitamin D is important in calcium and phosphate homeostasis in vertebrates, including regulation of the transcellular calcium uptake, cytosolic calcium transport, and modulation of the expression of Na^+-dependent P_i transporters, the main route of phosphate uptake in the intestine and reabsorption in the kidney (Pike, 1991, Bronner, 2009, Taketani et al., 1998). However, during the last decades it has become evident that the vitamin D endocrine system also has important roles in other biological processes, such as in muscle functioning, the immune system, cell proliferation, endobiotic metabolism, and cardiovascular physiology (Zittermann, 2003, Lips, 2006, Grant, 2006, Nurminen et al., 2019, Pike and Meyer, 2010, Sutton and MacDonald, 2003, Marino and Misra, 2019).

VDR share most of the common structural features found in other

* Corresponding author at: Department of Biological Sciences, University of Bergen, P.O. box 7803, 5020 Bergen, Norway.
E-mail address: odd.karlsen@uib.no (O.A. Karlsen).

https://doi.org/10.1016/j.aquatox.2021.105914
Received 4 December 2020; Received in revised form 6 July 2021; Accepted 13 July 2021
Available online 16 July 2021

members of the nuclear receptor superfamily, including two well-conserved core domains, the DNA-binding domain (DBD) and the ligand-binding domain (LBD) (McDonnell et al., 1989, Germain et al., 2006, Pawlak et al., 2012). The LBD is responsible for the binding of ligands to the ligand-binding pocket (LBP), and it contains a conserved motif important for dimerization to the retinoid X receptor (RXR), as well as the ligand dependent transactivation function (AF-2) for co-activator recruitment and binding (Moras and Gronemeyer, 1998). Following ligand activation by calcitriol, VDR can either form a homodimer and directly translocate to the nucleus, or heterodimerize with RXR before nuclear translocation (Carlberg et al., 1993, Nishikawa et al., 1994). In the nucleus, the VDR-VDR or VDR-RXR complex directs the cellular transcription machinery to the VDR response elements and initiates the transcription of VDR target genes (Dusso et al., 2005), including calcitriol-degrading enzymes, such as 25-hydroxyvitamin D-24-hydroxylase (CYP24A1) (Prosser and Jones, 2004, Jones et al., 2012). In fish, the conversion of 25(OH)D_3 to the metabolically active calcitriol takes place in the liver, as well as the kidney (Takeuchi et al., 1991, Lock et al., 2010, Graff et al., 1999), but some researchers have suggested that the liver is the main organ for synthesis of calcitriol in fish (Sundell et al., 1992, Takeuchi et al., 1991).

In contrast to mammals, which harbor only one VDR-encoding gene, teleosts possess two paralogs of Vdr[1], denoted Vdr alpha (Vdra) and Vdr beta (Vdrb). Vdra and Vdrb form distinct clades within teleost Vdr sequences, consistent with the notion of paralogous genes arising from the fish-specific whole genome duplication event that occurred before the radiation of teleost fishes (Kollitz et al., 2014, Howarth et al., 2008). The exact roles of the different Vdr paralogs in fish have not yet been elucidated. However, in some teleosts it has been demonstrated that Vdra and Vdrb exhibit different tissue-specific expression profiles and target gene repertoire, as well as different sensitivities to calcitriol, suggesting that Vdra and Vdrb have undergone a functional diversification through a process of sub- and/or neofunctionalization of Vdr gene pairs (Maglich et al., 2003, Howarth et al., 2008, Suzuki et al., 2000). A knock-down study performed in zebrafish (*Danio rerio*) with *vdr* morpholinos indicates involvement of drVdra in calcemic regulation, while drVdrb appeared to be nonfunctional in this process (Lin et al., 2012). On the other hand, drVdrb was reported to be the most important subtype for bone, inner ear, and heart development in zebrafish (Kwon, 2016a, Kwon, 2016b, Kwon, 2019).

Atlantic cod (*Gadus morhua*) is an ecologically and commercially important teleost species widely distributed in the North Atlantic Ocean. Atlantic cod has commonly been used as an indicator species in marine pollution monitoring programs, such as the OSPAR convention and water column monitoring of offshore petroleum activities in Norway (Hylland, 2006, Vethaak et al., 2017, Hylland et al., 2008). The habitat of Atlantic cod, including spawning and nursery grounds, coincide in many cases with areas with ongoing or planned off-shore petroleum activities, as well as coastal zones that are exposed to sewage discharges, runoff from roads, smelter industries, and accidental oil spills (Vikebø et al., 2014). Thus, this species is exposed to anthropogenic pollutants, including oil-related compounds such as polycyclic aromatic hydrocarbons (PAHs) shown to have significant impact on marine wildlife and ecosystems (Carls et al., 1998, Marty et al., 1997, Heintz et al., 1999, Pampanin and Sydnes, 2013). Crude oil and PAH exposures of Atlantic haddock and cod have been linked to bone deformities and cardiotoxicity (Sørhus et al., 2016, Sørhus et al., 2015, Sørensen et al., 2017) in embryos and larvae. While some effects have been associated with aryl hydrocarbon receptor (AHR/Ahr) activation, other studies report non-Ahr mediated PAH toxicities (Hodson, 2017, Incardona, 2017, Incardona et al., 2005, Incardona et al., 2004, Sørhus et al., 2016). It was demonstrated that cardiotoxicity of crude oil in Atlantic cod and haddock embryos was most likely due to Ahr-independent mechanisms since no activation of Ahr was observed in cardiomyocytes of the most severely impacted embryos (Sørhus et al., 2016). Notably, both cardiotoxicity and bone deformations are also two important phenotypes observed with vitamin D deficiency and in Vdr knockdown studies in zebrafish (Kwon, 2016b, Kwon, 2019). However, putative interactions between PAHs and the VDR/Vdr signaling pathway have so far not been extensively studied. Interestingly, several different compounds were found to activate or antagonize hsVDR in automated high-throughput screening assays performed as part of the Tox21 program (Dix et al., 2007, Collins et al., 2008), including the PAH 7-methylbenzo[a]pyrene (7mBaP) (Mahapatra et al., 2018).

Here we describe the primary structures, phylogeny, tissue specific expression, and agonistic activation of Atlantic cod Vdra (gmVdra) and Vdrb (gmVdrb) by calcitriol, and show that the calcitriol-mediated activation of gmVdrs can be modulated by PAHs. Homology modeling, docking analyses, and *in silico* solvent mapping studies indicated a putative second binding site for calcitriol and PAHs in the gmVdr protein structures that may contribute to the observed alteration of receptor activities. Thus, our data suggest that PAHs can interact with gmVdr receptors but require the presence of calcitriol in order to modulate their activity.

2. Methods

2.1. Sequence alignments and phylogenetic analyses

Multiple sequence alignments of full-length VDR/Vdr amino acid sequences were made with Clustal Omega and edited in Jalview (Jalview version 2.10.5). Sequence identity and sequence similarity scores were calculated by pairwise alignment of amino acid sequences using the Ident and Sim online tool (BLOSUM62 and value for internal gaps -2) (Stothard, 2000).

The phylogenetic analysis was performed using full-length VDR/Vdr amino acid sequences from a selected set of fishes, mammals, birds, and reptiles obtained from GenBank (Supplementary method 1.1). VDR/Vdr sequences were aligned with T-Coffee and the phylogenetic tree was constructed by Bayesian inference analysis using MrBayes v3.2.6. (See the supporting information for details) (Notredame et al., 2000, Ronquist and Huelsenbeck, 2003, J. P. Huelsenbeck and Ronquist., 2001).

2.2. Cloning of Atlantic cod Vdrs

Total RNA was extracted from Atlantic cod liver tissue (TriZol, Invitrogen, Carlsbad, CA) and cDNA was synthesized (Superscript III, Invitrogen). Nucleotide sequences encoding the hinge region and the LBD of Vdra (AA89-420) and Vdrb (AA89-425) were amplified by PCR (Takara ExTaq) using gene specific primers (Supplementary Table S2) and subcloned in pSC-A (Strataclone). BamHI and EcoRI sites introduced in the PCR were used to transfer Vdr encoding fragments into pCMX-GAL4 expression plasmids (Blumberg et al., 1998).

2.3. Tissue specific expression of gmvdra and gmvdrb

Atlantic cod from Havbruksstasjonen in Tromsø (Nofima, Norway) were kept at the Industrial and Aquatic Laboratorium (ILAB) in Bergen in 500 L tanks supplied with natural seawater at 8-10°C with a 12/12 h light/dark cycle regime. The fish were fed *ad libitum* with a commercial diet (Amber Neptun, Skretting, Stavanger, Norway). Female juvenile fish (104-131 g) were used in the tissue-specific expression study. Additionally, testis tissue was acquired from more mature Atlantic cod males (950-2805 g). Tissue samples were collected from ovary, muscle, head kidney, skin, mid intestine, spleen, heart, stomach, liver, brain, gill, eye ($n = 5$ juvenile Atlantic cod females) and testis ($n = 4$ Atlantic cod males) and snap frozen in liquid nitrogen. RNA was extracted with the RNeasy Universal Kit (Qiagen, Hilden, Germany), and 500 ng RNA was reverse-transcribed to cDNA using the iScript™ cDNA Synthesis Kit

[1] Protein formatting for fish; the first letter is uppercase (e.g., Vdr).

(Bio-Rad, Hercules, CA). Quantitative real-time polymerase chain reaction analyses were performed using the SsoAdvanced™ Universal SYBR® Green Supermix (Bio-Rad) and a CFX96 detection system (Bio-Rad). The expression of *gmvdra* and *gmvdrb* were normalized in each tissue using the reference genes *ubiquitin A-52 residue ribosomal protein fusion product 1* (*uba52*) and *ribosomal protein lateral stalk subunit P1* (*rplp1*), which have been shown to be stably expressed in multiple tissues of Atlantic cod (Olsvik et al., 2008). The geNorm software (v3.2) was used to calculate the normalization factor based on the geometric mean (Vandesompele et al., 2002). Statistical differences in expression levels between *gmvdra* and *gmvdrb* were assessed using paired t-test on log2-transformed data.

2.4. Cell culturing, luciferase reporter gene assay, and monitoring of cell viability

COS-7 cells were maintained in a humidified incubator at 37°C with 5% carbon dioxide (CO_2) in phenol red Dulbecco's modified Eagle medium (DMEM) supplemented with 10% fetal bovine serum (FBS), 1 mM sodium pyruvate, 4 mM L-glutamate, and 100 U/mL penicillin and streptavidin. The medium and additives were supplied by Sigma-Aldrich. When 80-90% confluency was reached, the cells were dissociated with 1x Trypsin-EDTA for further sub culturing (See supplementary method 1.2 for more information).

Ligand activation of gmVdra and gmVdrb was measured with a luciferase reporter gene assay in COS-7 cells transiently expressing the GAL4-DBD/gmVdr-LBD fusion protein following the same procedure as reported previously (Lille-Langøy et al., 2015). In short, the cells were seeded into 96-well plates (5000 cells/well) and cultured at 37°C throughout the whole assay. 24 h post seeding the cells were co-transfected with a plasmid mixture (100 ng/well) containing GAL4-UAS luciferase reporter plasmid (tk-(MH100)x4 luc), the pCMX-GAL4(DBD)-Vdr(LBD) receptor plasmid (2:1 reporter:receptor plasmid mass ratio), and a beta-galactosidase producing plasmid (pCMV-β-galactosidase) (TransIT®-LT1 Transfection Reagent, Mirus). Test compounds, including naphthalene (0-20 μM), phenanthrene (0-20 μM), fluorene (0-20 μM), chrysene (0-20 μM), pyrene (0-20 μM), benzo[a]pyrene (0-20 μM), 7-methyl-benzo[a]pyrene (0-20 μM), GW0742 (0-20 μM), and calcitriol (0-3 μM), were dissolved in DMSO (Sigma Aldrich) and added to exposure medium (high glucose DMEM supplemented with charcoal-stripped FBS (10%), sodium pyruvate (1 mM), L-glutamate (4 mM), and penicillin and streptavidin (100 U/mL)). After 24 h incubation, transfected cells were exposed for 24 h. The concentration of DMSO in exposure media were 0.5% (v/v) or less. Following exposure, cells were lysed and luciferase and beta-galactosidase activities were measured in lysates as luminescence and absorbance, respectively, using an Enspire Multimode plate reader (Perkin Elmer, Waltham, Massachusetts, USA). Dose-response curves were calculated by nonlinear regression (4 parameters, GraphPad Prism ver. 8) of fold changes in luciferase activity measured at different concentrations of test compounds relative to solvent control in 14 independent experiments for calcitriol and three independent experiments for the PAHs. EC_{50} values were estimated by determining the concentration at which 50% of maximal activation was achieved. Putative antagonistic and potentiating effects of PAH exposure were assessed with a slightly modified version of the luciferase reporter gene assay where a fixed concentration of 0.1 μM calcitriol (equaling approx. EC_{20-25}) were added to both solvent control and the test compounds. Statistical differences were assessed by comparing the luciferase activities in ligand exposed cells to solvent exposed cells (agonistic assay: DMSO; antagonistic/potentiating assay: DMSO and 0.1 μM calcitriol) by using ANOVA and Dunnett's multiple comparison test.

Cell viability assays were performed with COS-7 cells to assess putative cytotoxicity of the test compounds by measuring mitochondrial metabolic activity using the resazurin reduction method essentially as described by Pérez-Albaladejo (Pérez-Albaladejo et al., 2016) . The viability of exposed cells was compared to solvent exposed control cells in 2-3 independent experiments with 3 technical replicates. Statistical differences to control were assessed using Kruskal-Wallis non-parametric test in GraphPad Prism ver. 8.

2.5. Homology modelling and ligand docking

Homology models of the ligand-binding domain of gmVdra and gmVdrb were constructed using Modeller (v9.18; (Webb and Sali, 2014)) based on crystal structures of zebrafish Vdra (PDB: 2HC4, 3O1D, 4FHH, 4IA1, 4Q0A, 4RUJ, 5E7V, 5MX7, 5NKY, 5OW7, 5OW9, 5OWD (Otero et al., 2016, Lin et al., 2018, Belorusova et al., 2014, Belorusova et al., 2017) and human PXR (PDB: 6HJ2). In the homology models there is a region in the hinge area (gmVdra 158-216, gmVdrb 163-222) that is disordered in all the crystal structures, and thus cannot be modelled well. Docking of flexible ligands into models with rigid protein backbones and both rigid and flexible side chains was performed using Smina, with the Vinardo scoring function (Quiroga and Villarreal, 2016, Koes et al., 2013), retaining a broad range of calculated energies and a minimum of 10 modes.

Computational solvent mapping of small molecule fragments was performed using the FTMap server (Brenke et al., 2009), and visualized with Pymol (Schrödinger, 2015). Relative ligand positioning was analyzed in part with LigRMSD (Velazquez-Libera et al., 2020).

3. Results

3.1. Cloning, sequencing, and phylogenetic analyses of two Atlantic cod Vdrs

Homology searches in the Atlantic cod genome (gadMor3.0, GenBank assembly accession GCA_902167405.1) identified two predicted Vdr (Nr1i1) encoding genes (GeneID: LOC115551169 and LOC115556699). The coding sequences of these genes were cloned from cDNA prepared from Atlantic cod liver. DNA sequencing revealed that the cloned transcripts constitute two open reading frames consisting of 1257 bp and 1275 bp, encoding proteins with calculated molecular weights of 46.5 kDa (419 aa) and 47.2 kDa (425aa), respectively. The resulting nucleotide sequences were deposited in GenBank (National Center for Biotechnology Information) with the following accession numbers, MT344110 and MT344111.

A phylogenetic tree was constructed based on the deduced amino acid sequences and VDR/Vdr sequences obtained from a diverse group of vertebrate organisms, including a wide range of teleosts and selected amphibian, avian and mammalian species (Fig. 1). Importantly, the phylogeny shows a distinct clustering of MT344110 and MT344111 within the teleost Vdra and Vdrb clades, respectively, and they were accordingly named *gmvdra* and *gmvdrb*. The Atlantic cod genome was used for exon-intron mapping of the *gmvdr* genes, demonstrating that both *gmvdra* and *gmvdrb* consist of eight exons, which are located on chromosomes 1 and 13, respectively (Fig. 2A).

The paralogous gmVdra and gmVdrb amino acid sequences share a sequence similarity and identity of 96.0% and 86.6%, respectively (Fig. 2B). Sequence alignments also revealed a high degree of conservation between gmVdra and gmVdrb and orthologs from zebrafish and human, which previously have been thoroughly characterized (Fig. 2B) (Craig et al., 2008, Lin et al., 2012, Pike, 1991, Pike and Meyer, 2010, Baker et al., 1988). Between the Atlantic cod and zebrafish orthologs, the sequence identities corresponded to 89.6% and 88.8% for Vdra and Vdrb, respectively. As expected, gmVdra and gmVdrb are more diverged from the human ortholog, with amino acid identities corresponding to about 70% (Table S4). Furthermore, the gmVdr proteins share the common organization of nuclear receptors with a well-conserved DNA-binding domain, a hinge region, and a ligand-binding domain. The eight cysteine residues part of the zinc-finger motif are conserved, and conservation of the P-box, D-box, T-box, and A-box regions

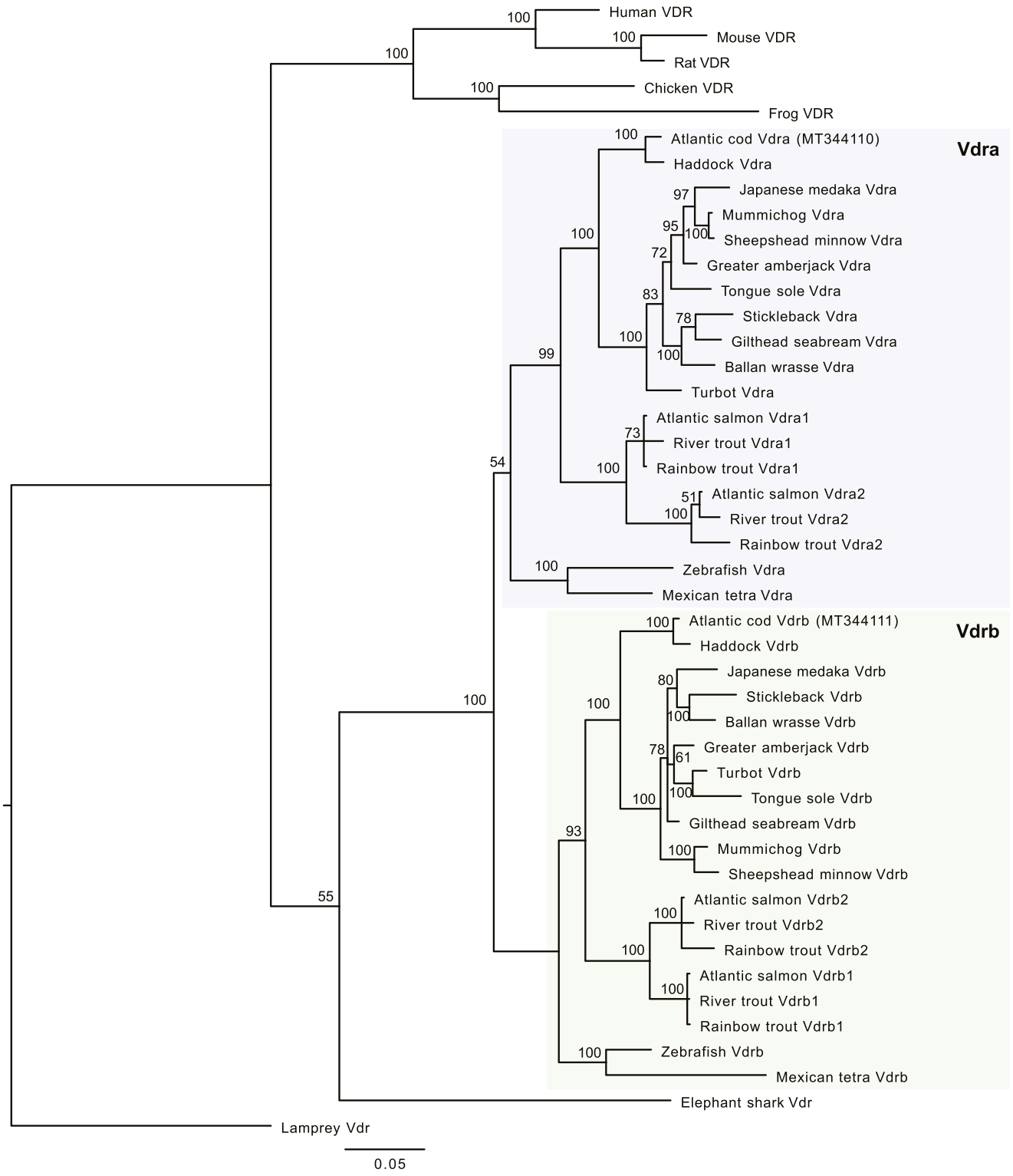

Fig. 1. Phylogenetic analyses of the Atlantic cod Vdr proteins and other vertebrate Vdr orthologs. The phylogenetic tree was created in MrBayes 3.2.6 using Blosum62 as substitution model. The Markov chain Monte Carlo (MCMC) analysis was run for 300000 generations for each 100 samples with a 25% burn-in. A selected set of full-length VDR/Vdr amino acid sequences from fish, amphibian, avian, and mammalian species were used, and their accession numbers are provided in Supplementary Table S1. Lamprey Vdr was used as an out-group to root the tree. Clade credibility values are indicated on each node.

important for DNA-binding specificity, homodimerization, and RXR heterodimerization, are mostly maintained in the gmVdr sequences (Kollitz et al., 2014, Hsieh et al., 1999, Umesono and Evans, 1989, Khorasanizadeh and Rastinejad, 2001, Rastinejad et al., 1995). All amino acid residues shown to be involved in the coordination and binding of calcitriol in human VDR (Väisänen et al., 2002) are positionally conserved in both gmVdra and gmVdrb (Fig. 2B) (Peleg and Nguyen, 2010).

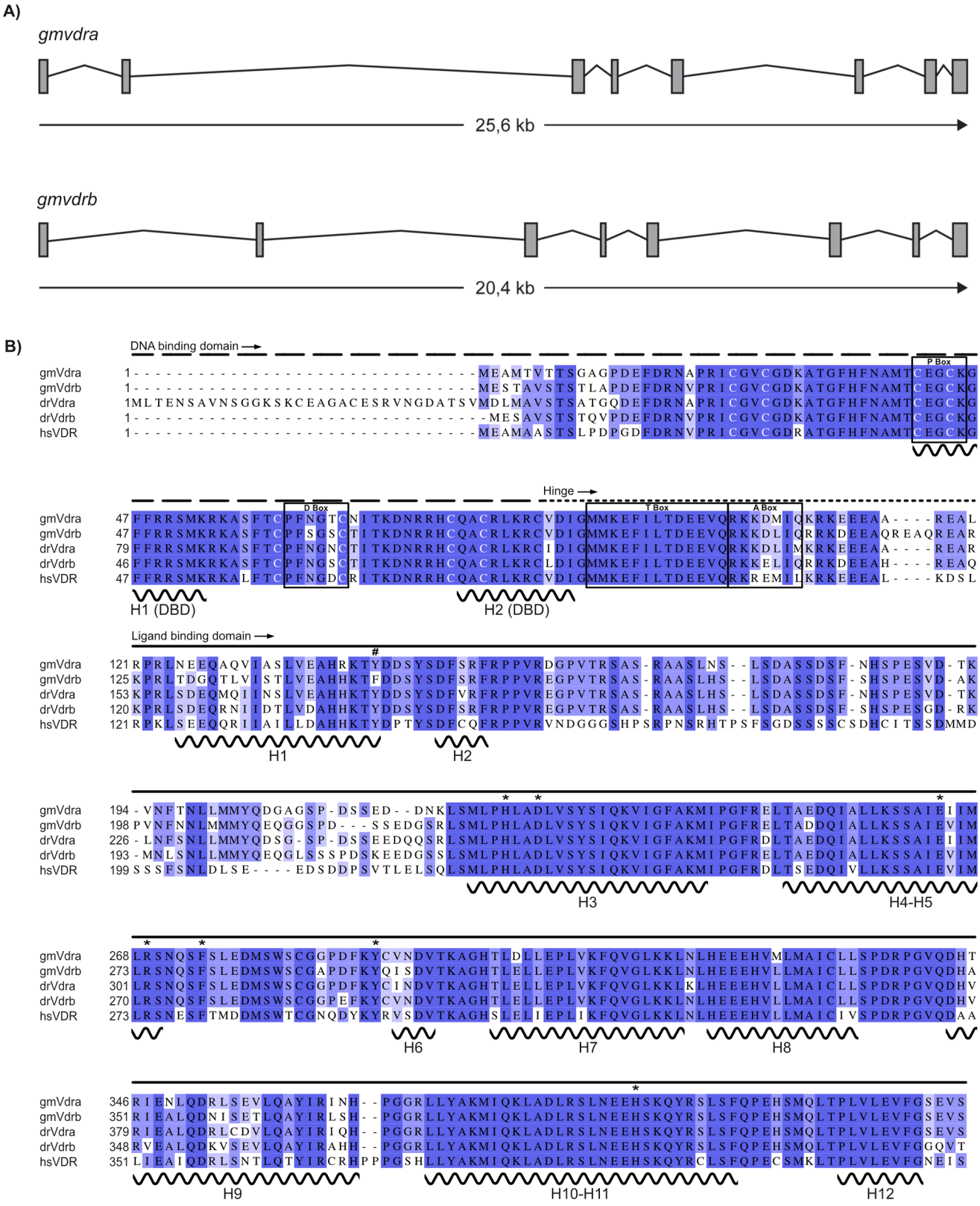

Fig. 2. Multiple sequence alignment and exon-intron mapping of Atlantic cod Vdr sequences. A) Exon-intron mapping of *gmvdra* and *gmvdrb* based on the most recent assembly of the Atlantic cod genome (gadMor3.0, GenBank assembly accession GCA_902167405.1, (Tørresen et al., 2017)). Exons are presented as grey boxes and introns as lines connecting the exons. B) Deduced amino acid sequences of *gmvdra* (MT344110) and *gmvdrb* (MT344111) were aligned with zebrafish drVdra, drVdrb, and human hsVDR using Clustal Omega. The alignment was manually edited in Jalview and amino acids are colored by % identity. Assignment of domains, secondary structure annotations (Kollitz et al., 2014, Kollitz et al., 2015), motifs, and key amino acids (Väisänen et al., 2002) are based on the human hsVDR ortholog. DNA binding domain (DBD), hinge region, and ligand-binding domain (LBD) are indicated with a scattered line, dotted line, and full line, respectively. Alpha helices are indicated below the alignment. Amino acids participating in binding of calcitriol are marked with asterisk, while the P, D, T, and A boxes, are indicated with squares. Cysteines important for zinc-finger formation are colored in white. # indicates the substitution of tyrosine to phenylalanine in the LBD of gmVdrb.

3.2. Tissue specific expression of gmvdra and gmvdrb

Tissue specific expression of *gmvdra* and *gmvdrb* was assessed in thirteen different tissues obtained from five female juvenile Atlantic cod, including ovary, muscle, head kidney, skin, mid intestine, spleen, heart, stomach, liver, brain, gill, and eye, as well as testis obtained from more mature male cod (Fig. 3). *gmvdra* and *gmvdrb* transcripts were ubiquitously expressed and identified in all tissues examined. In general, higher abundances of *gmvdra* relative to *gmvdrb* were observed in most tissues, apart from the ovaries where *gmvdrb* was most abundant. The highest expression levels of both paralogs were revealed in the liver, brain, and eye. Supplementary Fig. S1 shows the full tissue specific expression in the mature males.

3.3. Transactivation of Atlantic cod Vdrs by calcitriol

A luciferase reporter gene assay with COS-7 cells transiently expressing gmVdra or gmVdrb LBD fused to the Gal4-DBD was used to assess the activation of gmVdr by the endogenous ligand calcitriol. A dose-response dependent activation was observed for both gmVdr paralogs. However, the efficacy of calcitriol was significantly higher for gmVdra than for gmVdrb, corresponding to a maximum activation of 158- and 112-fold, respectively (Fig. 4). No significant difference in the potencies of calcitriol for the two paralogs was observed. The half maximal effective concentrations (EC_{50}) of calcitriol were estimated to be 0.21 μM and 0.24 μM for gmVdra and gmVdrb, respectively.

3.4. PAHs modulate the activity of Atlantic cod Vdr paralogs

A selected set of PAHs (Table S1) were tested for their ability to act as agonists for the gmVdr paralogs, including 7-methylbenzo[a]pyrene that previously was shown to act as an agonist of human VDR (Mahapatra et al., 2018) (Supplementary Fig. S2). However, no agonistic effects were observed in the gmVdr transactivation assays. To explore possible interactive effects of calcitriol and PAHs on the activity of gmVdra and gmVdrb, binary exposures of each PAH with a fixed concentration of calcitriol were performed (Fig. 5). Interestingly, COS-7 cells expressing gmVdra demonstrated a significant decrease in transactivation when co-exposed with calcitriol in combination with either phenanthrene, fluorene, pyrene, or the known weak mammalian VDR antagonist GW0742 (Fig. 5B, C, E, and H, respectively), suggesting that these PAHs may act as gmVdra antagonists. Although not statistically significant, similar antagonistic trends were observed with gmVdrb and the same PAHs. The cytotoxicity assays did not reveal any reduction in cell viabilities that could explain the observed decrease in calcitriol-mediated luciferase activity (Supplementary Fig. S3). Intriguingly, significant increases in both calcitriol-dependent Vdra and Vdrb activation were observed when co-exposing with calcitriol and either chrysene or benzo[a]pyrene, indicating that these compounds can potentiate the calcitriol-mediated Vdr activity (Fig. 5D and F). The strongest potentiating effects were observed with co-exposure of calcitriol and chrysene, which increased the receptor activities by approximately 125% and 167% for gmVdra and gmVdrb, respectively.

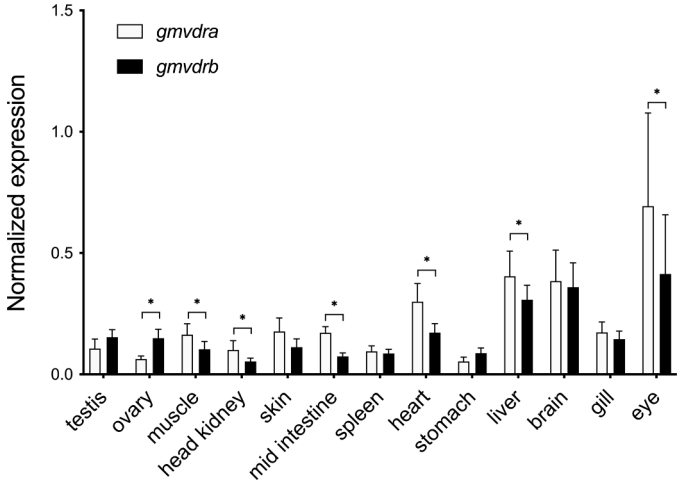

Fig. 3. Tissue specific distribution of *gmvdra* and *gmvdrb* transcripts in Atlantic cod. qPCR was used to assess the expression levels of *gmvdr* paralogs in ovary, muscle, head kidney, skin, mid intestine, spleen, heart, stomach, liver, brain, gill, and eye obtained from female juvenile Atlantic cod (n=5). In addition, testis tissue was obtained from more mature Atlantic cod males (n=4). Expression levels were normalized against the reference genes *uba52* and *rplp1*. Data is presented as normalized expression ± SEM. Statistical differences (* = $p < 0.05$) in expression levels between *gmvdra* and *gmvdrb* were assessed using paired t-test on log2-transformed data.

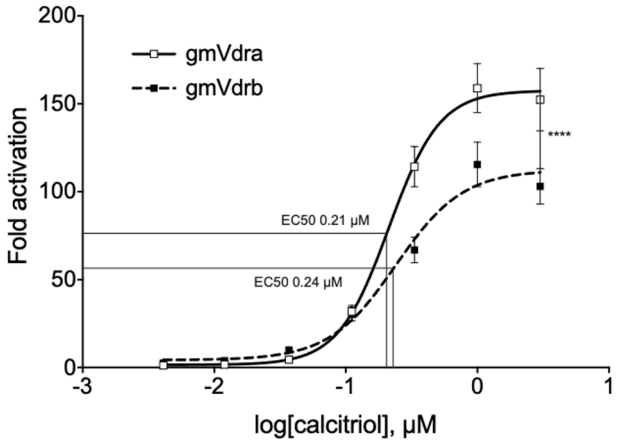

Fig. 4. Dose-response curve for activation of Atlantic cod Vdr paralogs by calcitriol. COS-7 cells transfected with gmVdra or gmVdrb were exposed to calcitriol at increasing concentrations (0.004-3 μM). Dose-response curves are presented as fold activation of the receptors in exposed cells compared to cells exposed to solvent control (0.03% DMSO). Data are presented as means ± SEM from 14 independent experiments (n=14), where each experiment included 3 technical replicates. Dose-response curves were calculated by nonlinear regression (4 parameters, GraphPad Prism ver. 8). Half maximal effective concentrations (EC_{50}) were estimated to be 0.21 μM (0.16-0.28 μM 95% CI) and 0.24 μM (0.17-0.34 μM 95% CI) for gmVdra and gmVdrb, respectively.

3.5. Homology modelling and solvent mapping analyses of gmVdra and gmVdrb

To further investigate the ligand binding properties of gmVdra and gmVdrb, homology models of the gmVdr paralogs were created using multiple crystal structures of zebrafish Vdra as templates. The constructed 3D models closely resemble the zebrafish Vdr structures, as there is a 91% amino acid identity between the available crystal structures and the Atlantic cod Vdr sequences. However, all available zebrafish Vdr crystal structures contain a disordered region near the N-terminal end of the LBD of about 67 amino acids, which is in a similar location to a disordered region of 59 amino acids in the rat and human VDR structures. Part of this region exhibits sequence similarity to human PXR (PDB ID 6HJ2), allowing us to construct a model containing additional loops not present in the available mammalian and teleost crystal structures.

With the constructed gmVdr models, *in silico* methods were used to evaluate the association properties of small molecules and ligands. Computational solvent mapping of billions of small molecular fragment probe positions can be used to determine binding 'hot-spots' (Kozakov et al., 2015, Hall and Enyedy, 2015, Ngan et al., 2009). Application of this method identified the canonical ligand-binding pocket, but also revealed an additional lower affinity binding site in a cleft on the

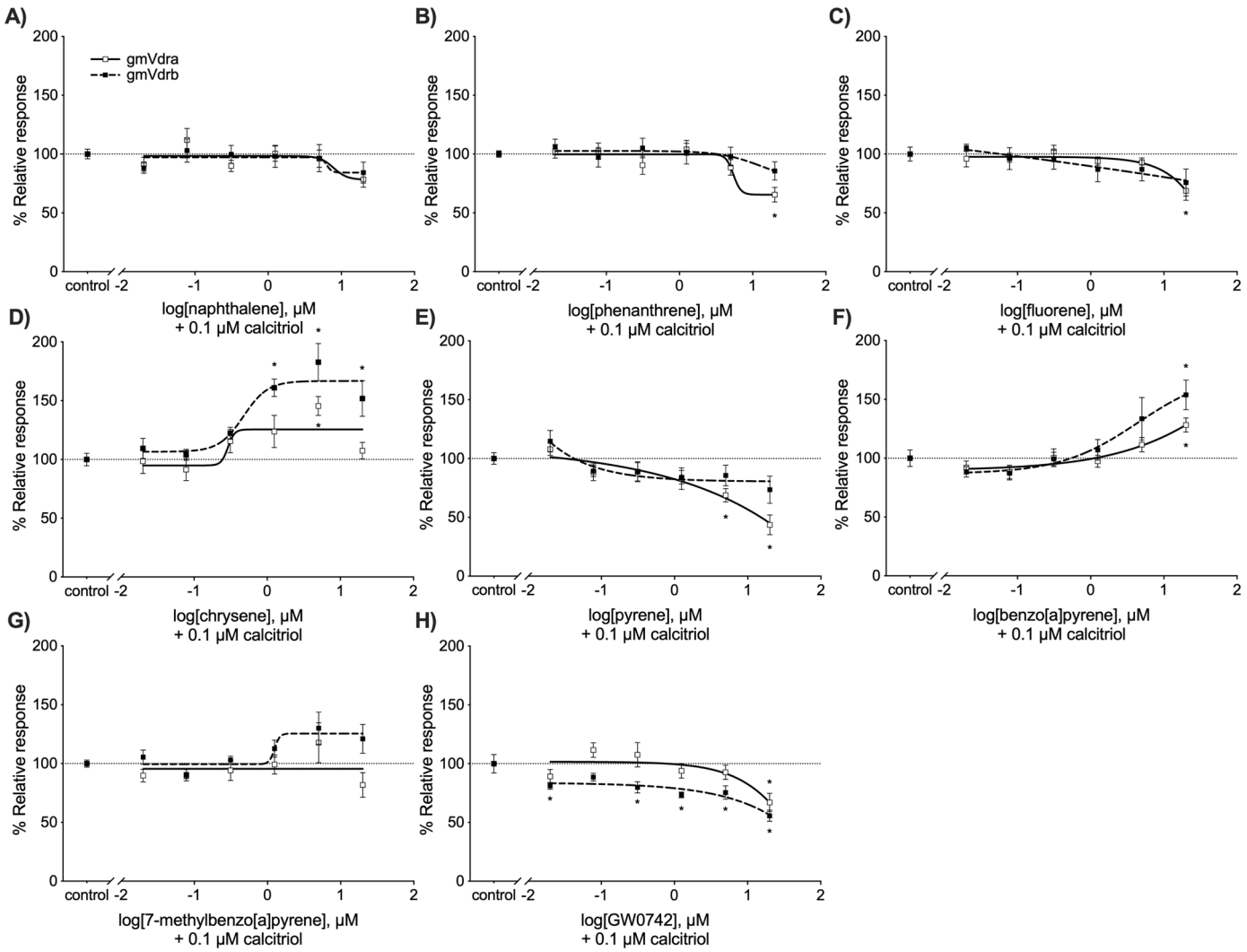

Fig. 5. Luciferase reporter gene assays with binary exposures of calcitriol and PAHs in COS-7 cells transiently expressing gmVdra and gmVdrb. COS-7 cells were exposed to a combination of 0.1 µM calcitriol and increasing concentrations of PAHs (0.02-20 µM) or the mammalian VDR antagonist GW0742 (0.02-20 µM) as indicated. A) naphthalene, B) phenanthrene, C) fluorene, D) chrysene, E) pyrene, F) BaP, G) 7mBaP, and H) GW0742. Responses in co-exposed cells are presented relative to responses in calcitriol exposed cells (adjusted to 100%) ± SEM from 3 independent experiments (n=3), where each experiment included 3 technical replicates. White and black squares represent responses mediated by gmVdra and gmVdrb, respectively. Asterisks (*) denote responses in co-exposed cells that differ significantly ($p<0.05$) from responses of calcitriol-exposed cells as calculated by ANOVA and Dunnett's multiple comparisons test.

surface, adjacent to the terminal helix 12 (which is the AF2 domain). Both Vdra (Fig. 6) and Vdrb (Supplementary Fig. S4) exhibited this additional binding hotspot.

Conventional ligand docking to homology models with flexible side chains provides an estimation of relative ligand docking. The top calcitriol docked position for gmVdra reproduced the ligand positioning of calcitriol analogs in zebrafish Vdr crystal structures, with an overall RMSD of less than 2 Å. Docking of a series of PAH compounds (Fig. 7) using Smina gave an order of relative affinity of calcitriol > GW0742> chrysene > BaP ~ 7-methylBaP ~ pyrene ~ fluorene ~ phenanthrene > naphthalene (Table 1). Using static amino acid sidechains maintain this order but decreases the calculated affinities (data not shown). Note that these calculated energies do not clearly correspond to ligand affinities (or Kd values), but they do provide a scoring guide to ligand association with proteins. Computational ligand associations do not necessarily indicate agonism, and in this case could indicate antagonism. The crystal structures used for homology modeling all include co-crystalized ligands, and thus represent closed putatively active receptors. Little significant differences were noted in calculated affinities between gmVdra and gmVdrb, except a slightly lower affinity of gmVdrb for calcitriol. PAH ligands docked in both 'branches' of the Vdr LBD, with calcitriol occupying the center of the main LBP (including in cross-docking). However, we did observe ligand binding to the alternative hot-spot indicated by the computational solvent docking for calcitriol and with lesser affinity, 7-methylBaP. Cross-docking of PAH molecules with the calcitriol-bound Vdr structures also led to docking in the alternative hot-spot.

4. Discussion

The two paralogous Vdr-encoding genes in the Atlantic cod genome grouped phylogenetically within the teleost fish Vdra and Vdrb subfamilies. The structural organization of VDR/Vdr is well maintained across vertebrates, including the positional conservation of the calcitriol-binding amino acids in the LBP. Accordingly, both gmVdra and gmVdrb were transactivated by calcitriol in the luciferase reporter gene assay, but distinct differences in efficacies were observed. The calcitriol-induced response in COS-7 cells expressing gmVdra was stronger than in cells expressing gmVdrb (158-fold (95% CI: 143-174-fold) compared to 112-fold (95% CI: 100-128-fold)). Possible differences in the binding of

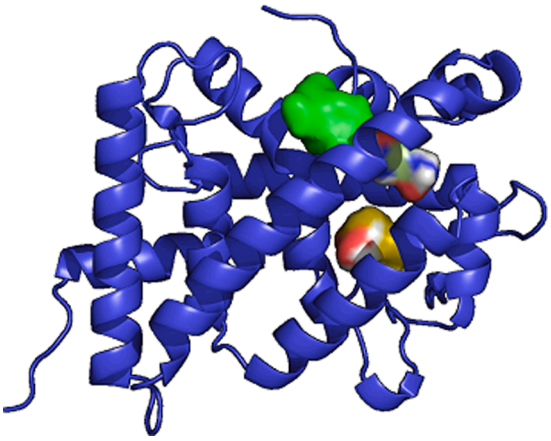

Fig. 6. Solvent mapping of Atlantic cod Vdra predicted protein structure. Solvent mapping of small molecular fragments shows hot spots of ligand affinity both in the LBD and in an exposed surface cleft of gmVdra. The solvent fragments docking into the LBD are variously colored, while the cleft hot spot is colored green.

calcitriol were also indicated in the docking analyses with the gmVdr homology models, where Vdrb demonstrated slightly lower affinity towards calcitriol. However, calcitriol seemed to be an equally potent agonist for the two Atlantic cod Vdrs (EC_{50}: 0.21 μM (160-280 nM 95% CI) and 0.24 μM (170-340 nM 95% CI) for gmVdra and gmVdrb, respectively). Similar differences in efficacies in responses to calcitriol have previously been observed for Vdr paralogs from other teleost species, such as zebrafish, medaka (*Oryzias latipes*), and pufferfish (*Tetraodon nigroviridis*), where calcitriol-mediated transactivation via Vdrb produced considerably lower efficacy than Vdra (Kollitz et al., 2014). In gmVdrb, a substitution is observed at amino acid position 147, where a tyrosine (Y) is substituted with phenylalanine (F) (Y147F) compared to the other VDR/Vdr sequences (Fig. 2B, indicated by #). This amino acid was previously reported to be important for protein folding of human hsVDR and/or for the hydrogen bonding with the 3β-hydroxyl group on calcitriol, and the calcitriol transactivation was significantly reduced when this tyrosine was substituted with an alanine or phenylalanine (Choi et al., 2003, Mizwicki et al., 2004). The Y143F substitution in gmVdrb may thus contribute to the lower efficacy that was observed for gmVdrb compared to gmVdra. This difference is also reflected in the docking results (Table 1), as the docked calcitriol binding position is nearly perfectly superimposed on the calcitriol position in the zebrafish crystal structures and shows the interaction between the 3β-hydroxyl of calcitriol and Y147.

Table 1
Calculated ligand rankings and energy scores for authentic and PAH ligands of gmVdra and gmVdrb. Docking was performed using the Vinardo scoring function in Smina.

Ligand	Energy score (kcal/mol)	
	gmVdra	***gmVdrb***
calcitriol	-11.4	-10.5
GW0742	-10.5	-10.1
chrysene	-9.4	-8.7
BaP	-9.1	-8.9
pyrene	-8.9	-8.4
7-methylBaP	-8.8	-8.9
fluorene	-8.6	-8.0
phenanthrene	-8.6	-8.3
naphthalene	-7.2	-6.8

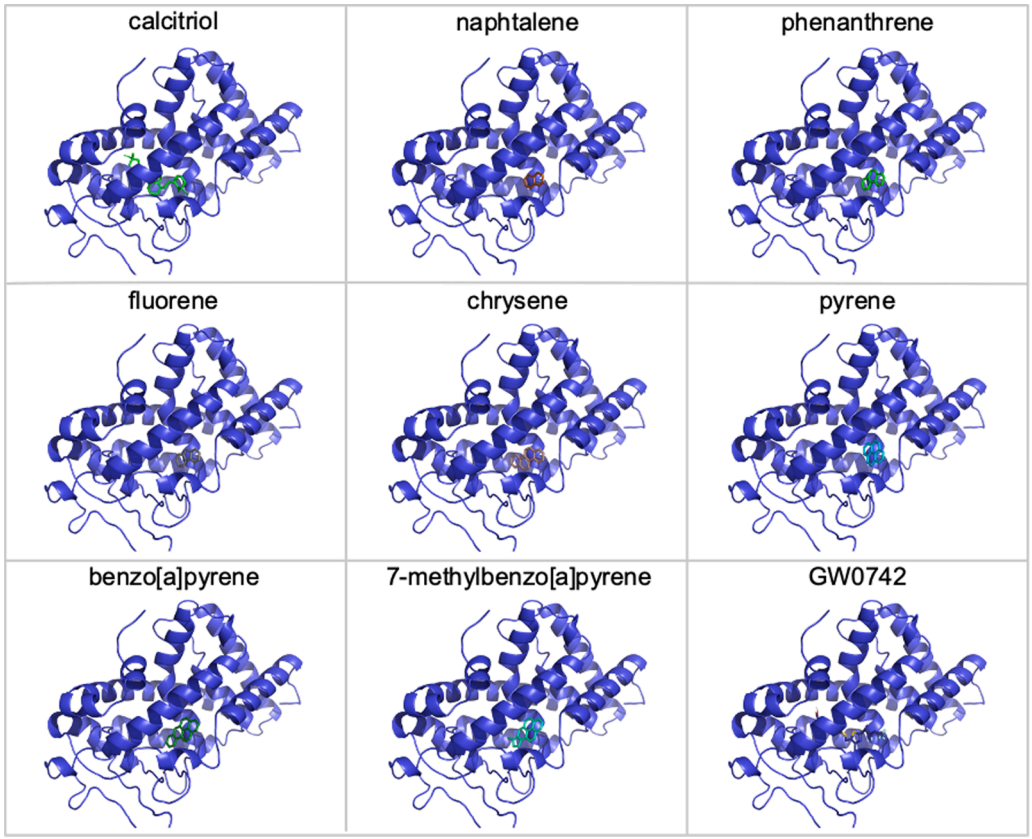

Fig. 7. Docking of ligands to Atlantic cod Vdra. PAH molecules occupy the primary ligand-binding pocket. Calcitriol docks to the primary pocket, but also occupies a secondary site in an exposed cleft (green region in Figure 6), in the same location determined to be a ligand-binding hotspot by the computational solvent mapping. Similar results are obtained with gmVdrb (Supplementary Figure S4).

Variation in reported EC_{50}-values among Vdr orthologs activated by calcitriol suggests differences in potencies across species; 5.38 nM (4.32-6.68 nM 95% CI) for human VDR, 2.61 nM for sea lamprey (*Petromyzon marinus*) Vdr, 7.93 nM for little skate (*Leucoraja erinacea*) Vdr, and 98.92 nM for Senegal bichir (*Polypterus senegalus*) Vdr (Kollitz et al., 2014, Kollitz et al., 2015). The calcitriol EC_{50}-values determined for the gmVdrs were approximately 100-fold higher than those reported for medaka and zebrafish (2.6 nM and 2.5 nM for zebrafish Vdra and Vdrb, respectively, and 2.6 nM and 3.1 nM for medaka Vdra and Vdrb, respectively) (Kollitz et al., 2014). However, it cannot be excluded that these discrepancies are caused by methodological differences in the reporter gene assays that were used. In the studies reported by (Kollitz et al., 2014), the full-length (i.e. including the DNA-binding domain) Vdra and Vdrb receptors from zebrafish and medaka were transiently expressed in HepG2 cells together with a xenobiotic reporter enhancer module of CYP3A4 (XREM-Luc). Caution must therefore be taken when comparing EC_{50}-values across experiments and species where different reporter gene assays have been used.

Tissue-specific expression analyses showed that both *gmvdra* and *gmvdrb* were ubiquitously expressed in most juvenile tissues examined. Furthermore, *gmvdra* exhibited stronger expression in the majority of tissues in comparison to *gmvdrb*. The ubiquitous expression of the *gmvdr* paralogs, as well as *gmvdra* being the subtype that is predominantly expressed in most tissues, are in agreement with studies on other fish (Howarth et al., 2008, Maglich et al., 2003, Suzuki et al., 2000, Peng et al., 2017). Moreover, the abundant expression of the *gmvdr* paralogs in eye, brain, and liver is also in accordance with tissue-specific expression profiles reported from other teleost species (Howarth et al., 2008, Maglich et al., 2003). Importantly, our findings substantiate that subfunction partitioning for gene expression of the Atlantic cod Vdr paralogs has occurred at the gross anatomical level as previously also suggested for the medaka Vdrs (Howarth et al., 2008).

Screening analyses of 400 compounds with putative VDR activity in the Tox21 qHTS dataset demonstrated that about 10% of these had the potential to modulate the activity of hsVDR, either as an agonist or antagonist (Mahapatra et al., 2018). While the PAH 7-methyl benzo[a] pyrene was one of the agonists identified among the compounds tested, our results show that 7mBaP does not act as an agonist for Atlantic cod Vdrs *in vitro*. In fact, none of the PAHs tested in this study activated the gmVdrs on their own (Supplementary information, Fig. S2). On the other hand, we observed interactions between PAHs and calcitriol that modulated the transcriptional activities of the gmVdr paralogs. Antagonistic effects were produced by phenanthrene, fluorene, and pyrene towards gmVdra, suggesting that these PAHs can suppress calcitriol-mediated receptor activation. Although fluorene and pyrene appear to cause some reduction in cell viability, this effect is not significant, and not directly parallel with the reduction in luciferase activity for the two gmVdrs. Hence, the data indicate a real antagonism of phenanthrene, and possibly also of fluorene and pyrene. Notably, pyrene produced stronger antagonistic effects in comparison to the mammalian VDR antagonist, GW0742. In contrast, chrysene and BaP demonstrated potentiating effects on the calcitriol-mediated activation of both gmVdra and gmVdrb, although BaP did cause a significant reduction in cell viability.

In silico ligand docking analyses supported that the PAHs assessed are capable of binding to the gmVdr LBDs. Several studies have shown that a nuclear receptor antagonist may bind to the LBD in similar ways as an agonist while not being able to stabilize an active conformation of the receptor (Moras and Gronemeyer, 1998) (Sakkiah et al., 2018). However, the exact mechanisms of how the PAHs antagonize or potentiate the activity of calcitriol in cod Vdrs remain to be elucidated. Interestingly, chrysene and B[a]P were the two congeners that were predicted to bind with the highest affinities. At the same time, these two PAHs were the only two PAHs tested that demonstrated a potentiating effect. Nonetheless, solvent-mapping analyses identified a putative second binding site located to a cleft on a surface between helix 11, helix 12, and helix 4-5. Similarly, a crystal structure of drVdra together with lithocholic acid (LCA) demonstrated that two possible binding sites in the LBD exist, one being the LBP and the other being characterized as a surface interaction between helix 2 and 3 (Belorusova et al., 2014). Docking analyses indicated that both calcitriol and PAHs could bind to this second binding site in the gmVdrs. Its location adjacent to helix 12 and the AF2 domain is interesting, as the AF2 domain interacts with the key partner protein nuclear receptor coactivator 1 (NCOA1/SRC1) (Westin et al., 1998), and interactions taking place in this region may thus influence the transcriptional activity of the gmVdrs.

Several studies have identified PAHs to be linked to cardiotoxicity and bone deformities in fish and other vertebrates, and both Ahr-dependent and Ahr-independent mechanisms have been described (Sestak et al., 2018, Cypher et al., 2017, Incardona et al., 2005, Sørhus et al., 2016, Sørensen et al., 2017, Jayasundara et al., 2015, Incardona et al., 2011). Cardiotoxicity and bone deformations are also phenotypes observed when the vitamin D signaling pathway is perturbed, such as with vitamin D deficiency and in Vdr knockdown studies in zebrafish (Lin et al., 2012, Kwon, 2019, Kwon, 2016b). Moreover, functional analyses identified drVdrb to be important for heart development (Kwon, 2016b), while both drVdra and drVdrb were important for correct craniofacial development (Kwon, 2019). Although none of the PAHs assessed were able to agonistically activate the Atlantic cod Vdr receptors, some of the PAHs, including phenanthrene, fluorene, pyrene, chrysene, and BaP antagonized or potentiated the calcitriol-mediated Vdr activation *in vitro*. The influence of these PAHs on Vdr activities may suggest that modulation of the vitamin D signaling pathway could be a contributing factor to the adverse effects induced by PAH exposures during early life stages of fish, including morphological abnormalities such as cardiotoxicity and bone deformities, which in teleosts appear to rely on a functional vitamin D metabolism for correct development (Lin et al., 2012, Kwon, 2019). Notably, an increased expression of the Vdr target gene *cyp24a* was recently found in Atlantic cod larvae exposed to crude oil, suggesting that PAHs, or other compounds present in crude oil, can modulate the vitamin D signaling pathway *in vivo* (Libe Aranguren-Abadía, personal information). A role of VDR in the response to PAHs has also been suggested previously in mammalian models (Berntssen et al., 2015, Matsunawa et al., 2012). For example, a combined exposure of BaP and calcitriol increased the CYP1A protein levels and activity in human macrophages to a larger extent than exposure to BaP alone, indicating that hsVDR could have a role in the biotransformation of PAHs and BaP-induced toxicity (Matsunawa et al., 2012). However, more studies are needed to further elucidate and confirm a potential role of Vdr in PAH-mediated toxicities and the putative implications of modulating Vdr activity *in vivo* in Atlantic cod.

Author statement

OAK and AG conceptualized the study. SØG, AG, and OAK developed the experimental design, and SØG conducted the experiments. JG contributed with homology modelling and ligand docking analyses. RL-L was involved in gene cloning, sequence analyses, and establishing the luciferase reporter gene assays. PAO was involved in analyses of qPCR-data. SØG, OAK, AG, JG, E-JL, and PAO wrote the manuscript, with SØG as the lead author. All authors contributed with revision of the manuscript.

Declaration of competing interest

There are no conflicts of interests to declare.

Acknowledgements

This study was funded by the Research Council of Norway through the "iCod 2.0: Integrative environmental genomics of Atlantic cod" project (project no. 244564) and the "dCod 1.0: decoding systems

toxicology of Atlantic cod" project (Center for Digital Life Norway project no. 248840). We thank the national cod breeding program in Norway, Nofima, for providing farmed Atlantic cod for this project. We would also like to thank Elisabeth Ueland and Ina Blindheim Johansen for the contributions made through their master theses on the vitamin D receptor from Atlantic cod, as well as Rhîan Gaenor Jacobsen for technical assistance in the laboratory.

Supplementary materials

Supplementary material associated with this article can be found, in the online version, at doi:10.1016/j.aquatox.2021.105914.

References

Adachi, R., Honma, Y., Masuno, H., Kawana, K., Shimomura, I., Yamada, S., Makishima, M., 2005. Selective activation of vitamin D receptor by lithocholic acid acetate, a bile acid derivative. J. Lipid Res. 46, 46–57.

Adachi, R., Shulman, A.I., Yamamoto, K., Shimomura, I., Yamada, S., Mangelsdorf, D.J., Makishima, M., 2004. Structural determinants for Vitamin D receptor response to endocrine and xenobiotic signals. Mol. Endocrinol. 18, 43–52.

Baker, A.R., McDonnell, D.P., Hughes, M., Crisp, T.M., Mangelsdorf, D.J., Haussler, M.R., Pike, J.W., Shine, J., O'Malley, B.W., 1988. Cloning and expression of full-length cDNA encoding human vitamin D receptor. Proc. Natl. Acad. Sci. 85, 3294–3298. 10.1073/pnas.85.10.3294.

Belorusova, A.Y., Eberhardt, J., Potier, N., Stote, R.H., Dejaegere, A., Rochel, N., 2014. Structural insights into the molecular mechanism of vitamin D receptor activation by lithocholic acid involving a new mode of ligand recognition. J. Med. Chem. 57, 4710–4719.

Belorusova, A.Y., Martinez, A., Gandara, Z., Gomez, G., Fall, Y., Rochel, N., 2017. Structure-activity relationship study of vitamin D analogs with oxolane group in their side chain. Eur. J. Med. Chem. 134, 86–96.

Berntssen, M.H.G., Ørnsrud, R., Hamre, K., Lie, K.K., 2015. Polyaromatic hydrocarbons in aquafeeds, source, effects and potential implications for vitamin status of farmed fish species: a review. Aquacult. Nutr. 21, 257–273.

Blumberg, B., Sabbagh, W., Juguilon, H., Bolado, J., van Meter, C.M., Ong, E.S., Evans, R. M., 1998. SXR, a novel steroid and xenobiotic-sensing nuclear receptor. Genes Dev. 12, 3195–3205.

Brenke, R., Kozakov, D., Chuang, G.Y., Beglov, D., Hall, D., Landon, M.R., Mattos, C., Vajda, S., 2009. Fragment-based identification of druggable 'hot spots' of proteins using Fourier domain correlation techniques. Bioinformatics 25, 621–627.

Bronner, F., 2009. Recent developments in intestinal calcium absorption. Nutr. Rev. 67, 109–113.

Carlberg, C., Bendik, I., Wyss, A., Meier, E., Sturzenbecker, L.J., Grippo, J.F., Hunziker, W., 1993. Two nuclear signalling pathways for vitamin D. Nature 361.

Carls, M.G., Rice, S.D., Hose, E., 1998. Sensitivity of fish embryos to weathered crude oil: Part I. Low-level exposure during incubation causes malformations, genetic damage, and mortality in larval pacific herring (Clupea pallasi). Environ. Toxicol. Chem. 18, 481–493.

Choi, M., Yamamoto, K., Itoh, T., Makishima, M., Mangelsdorf, D.J., Moras, D., DeLuca, H.F., Yamada, S., 2003. Interaction between Vitamin D Receptor and Vitamin D Ligands. Chem. Biol. 10, 261–270.

Collins, F.S., Gray, G.M., Bucher, J.R., 2008. Toxicology. Transforming environmental health protection. Science 319, 906–907.

Craig, T.A., Sommer, S., Sussman, C.R., Grande, J.P., Kumar, R., 2008. Expression and regulation of the vitamin D receptor in the zebrafish, Danio rerio. J. Bone Miner. Res. 23, 1486–1496. https://doi.org/10.1359/jbmr.080403.

Cypher, A.D., Consiglio, J., Bagatto, B., 2017. Hypoxia exacerbates the cardiotoxic effect of the polycyclic aromatic hydrocarbon, phenanthrene in Danio rerio. Chemosphere 183, 574–581.

Dix, D.J., Houck, K.A., Martin, M.T., Richard, A.M., Setzer, R.W., Kavlock, R.J., 2007. The ToxCast program for prioritizing toxicity testing of environmental chemicals. Toxicol. Sci. 95, 5–12.

Dusso, A.S., Brown, A.J., Slatopolsky, E., 2005. Vitamin D. 289, F8–F28.

Germain, P., Staels, B., Dacquet, C., Spedding, M., Laudet, V., 2006. Overview of nomenclature of nuclear receptors. Pharmacol. Rev. 58, 685–704.

Graff, I.E., Lie, Ø., Aksnes, L., 1999. In vitro hydroxylation of vitamin D3 and 25-hydroxy vitamin D3 in tissues of Atlantic salmon Salmo salar, Atlantic mackerel Scomber scombrus, Atlantic halibut Hippoglossus hippoglossus and Atlantic cod Gadus morhua. Aquacult. Nutr. 5, 23–32.

Grant, W.B., 2006. Epidemiology of disease risks in relation to vitamin D insufficiency. Prog. Biophys. Mol. Biol. 92, 65–79.

Hall, D.R., Enyedy, I.J., 2015. Computational solvent mapping in structure-based drug design. Future Med Chem 7, 337–353.

Heintz, R.A., Short, J.W., Rice, S.D., 1999. Sensitivity of fish embryos to weathered crude oil: Part II. Increased mortality of pink salmon (Oncorhynchus gorbuscha) embryos incubating downstream from weathered Exxon valdez crude oil. Environ. Toxicol. Chem. 18, 494–503.

Hodson, P.V., 2017. The toxicity to fish embryos of PAH in crude and refined oils. Arch. Environ. Contam. Toxicol. 73, 12–18.

Howarth, D.L., Law, S.H.W., Barnes, B., Hall, J.M., Hinton, D.E., Moore, L., Maglich, J. M., Moore, J.T., Kullman, S.W., 2008. Paralogous Vitamin D receptors in teleosts: transition of nuclear receptor function. Endocrinology 149, 2411–2422.

Hsieh, J.-C., Whitfield, G.K., Oza, A.K., Dang, H.T.L., Price, J.N., Galligan, M.A., Jurutka, P.W., Thompson, P.D., Haussler, C.A., Haussler, M.R., 1999. Characterization of unique DNA-binding and transcriptional-activation functions in the Carboxyl-Terminal extension of the zinc finger region in the human Vitamin D receptor. Biochemistry 38, 16347–16358.

Huelsenbeck, J.P., Ronquist., F, 2001. MRBAYES: Bayesian inference of phylogenetic trees. Bioinformatics 17, 754–755.

Hylland, K., 2006. Polycyclic Aromatic Hydrocarbon (PAH) ecotoxicology in marine ecosystems. J. Toxicol. Environ. Health Part A 69, 109–123.

Hylland, K., Tollefsen, K.-E., Ruus, A., Jonsson, G., Sundt, R.C., Sanni, S., Utvik, T., Johnsen, S., Nilssen, I., Pinturier, L., Balk, L., Baršienė, J., Marigòmez, I., Feist, S.W., Børseth, J., 2008. Water column monitoring near oil installations in the North Sea 2001–2004. Mar. Pollut. Bull. 56, 414–429.

Incardona, J.P., 2017. Molecular mechanisms of crude oil developmental toxicity in fish. Arch. Environ. Contam. Toxicol. 73, 19–32.

Incardona, J.P., Carls, M.G., Teraoka, H., Sloan, C.A., Collier, T.K., Scholz, N.L., 2005. Aryl hydrocarbon receptor–independent toxicity of weathered crude oil during fish development. Environ. Health Perspect. 113, 1755–1762.

Incardona, J.P., Collier, T.K., Scholz, N.L., 2004. Defects in cardiac function precede morphological abnormalities in fish embryos exposed to polycyclic aromatic hydrocarbons. Toxicol. Appl. Pharmacol. 196, 191–205.

Incardona, J.P., Linbo, T.L., Scholz, N.L., 2011. Cardiac toxicity of 5-ring polycyclic aromatic hydrocarbons is differentially dependent on the aryl hydrocarbon receptor 2 isoform during zebrafish development. Toxicol. Appl. Pharmacol. 257, 242–249.

Jayasundara, N., Van Tiem Garner, L., Meyer, J. N., Erwin, K. N. & Di Giulio, R. T. 2015. AHR2-mediated transcriptomic responses underlying the synergistic cardiac developmental toxicity of PAHs. 143, 469-481.

Jones, G., Prosser, D.E., Kaufmann, M., 2012. 25-Hydroxyvitamin D-24-hydroxylase (CYP24A1): its important role in the degradation of vitamin D. Arch. Biochem. Biophys. 523, 9–18.

Khorasanizadeh, S., Rastinejad, F., 2001. Nuclear-receptor interactions on DNA-response elements. Trends Biochem. Sci. 26, 384–390.

Koes, D.R., Baumgartner, M.P., Camacho, C.J., 2013. Lessons Learned in Empirical Scoring with smina from the CSAR 2011 Benchmarking Exercise. J. Chem. Inf. Model. 53, 1893–1904.

Kollitz, E.M., Hawkins, M.B., Whitfield, G.K., Kullman, S.W., 2014. Functional diversification of vitamin D receptor paralogs in teleost fish after a whole genome duplication event. Endocrinology 155, 4641–4654.

Kollitz, E.M., Zhang, G., Hawkins, M., Whitfield, K.G., Reif, D.M., Kullman, S.W., 2015. Molecular cloning, functional characterization, and evolutionary analysis of Vitamin D receptors isolated from basal vertebrates. PLoS One 10.

Kozakov, D., Grove, L.E., Hall, D.R., Bohnuud, T., Mottarella, S.E., Luo, L., Xia, B., Beglov, D., Vajda, S., 2015. The FTMap family of web servers for determining and characterizing ligand-binding hot spots of proteins. Nat. Protoc. 10, 733–755.

Krasowski, M.D., Ai, N., Hagey, L.R., Kollitz, E.M., Kullman, S.W., Reschly, E.J., Ekins, S., 2011a. The evolution of farnesoid X, vitamin D, and pregnane X receptors: insights from the green-spotted pufferfish (Tetraodon nigriviridis) and other non-mammalian species. BMC Biochem. 12, 5.

Kwon, H.-J., 2016a. Vitamin D receptor deficiency impairs inner ear development in zebrafish. Biochem. Biophys. Res. Commun. 478, 994–998.

Kwon, H.-J., 2016b. Vitamin D receptor signaling is required for heart development in zebrafish embryo. Biochem. Biophys. Res. Commun. 470, 575–578.

Kwon, H.-J., 2019. Vitamin D Receptor Signaling Regulates Craniofacial Cartilage Development in Zebrafish. J. Dev. Biol. 7, 13.

Lille-Langøy, R., Goldstone, J.V., Rusten, M., Milnes, M.R., Male, R., Stegeman, J.J., Blumberg, B., Goksoyr, A., 2015. Environmental contaminants activate human and polar bear (Ursus maritimus) pregnane X receptors (PXR, NR1I2) differently. Toxicol. Appl. Pharmacol. 284, 54–64.

Lin, C.-H., Su, C.-H., Tseng, D.-Y., Ding, F.-C., Hwang, P.-P., 2012. Action of Vitamin D and the receptor, VDRa, in Calcium Handling in Zebrafish (Danio rerio). PLoS One 7.

Lin, Z., Marepally, S.R., Goh, E.S.Y., Cheng, C.Y.S., Janjetovic, Z., Kim, T.K., Miller, D.D., Postlethwaite, A.E., Slominski, A.T., Tuckey, R.C., Peluso-Iltis, C., Rochel, N., Li, W., 2018. Investigation of 20S-hydroxyvitamin D3 analogs and their 1alpha-OH derivatives as potent vitamin D receptor agonists with anti-inflammatory activities. Sci. Rep. 8, 1478.

Lips, P., 2006. Vitamin D physiology. Prog. Biophys. Mol. Biol. 92, 4–8.

Lock, E.J., Waagbø, R., Wendelaar Bonga, S., Flik, G., 2010. The significance of vitamin D for fish: a review. Aquacult. Nutr. 16, 100–116.

Maglich, J.M., Caravella, J.A., Lambert, M.H., Willson, T.M., Moore, J.T., Ramamurthy, L., 2003. The first completed genome sequence from a teleost fish (Fugu rubripes) adds significant diversity to the nuclear receptor superfamily. Nucleic. Acids. Res. 31, 4051–4058.

Mahapatra, D., Franzosa, J.A., Roell, K., Kuenemann, M.A., Houck, K.A., Reif, D.M., Fourches, D., Kullman, S.W., 2018. Confirmation of high-throughput screening data and novel mechanistic insights into VDR-xenobiotic interactions by orthogonal assays. Sci. Rep. 8, 8883.

Makishima, M., Lu, T.T., Xie, W., Whitfield, G.K., Domoto, H., Evans, R.M., Haussler, M. R., Mangelsdorf, D.J., 2002. Vitamin D receptor as an intestinal bile acid sensor. Science 296, 1313–1316.

Marino, R., Misra, M., 2019. Extra-skeletal effects of Vitamin D. Nutrients 11, 1460.

Marty, G.D., Hinton, D.E., Short, J.W., Heintz, R.A., Rice, S.D., Dambach, D.M., Willits, N.H., Stegeman, J.J., 1997. Ascites, premature emergence, increased gonadal cell apoptosis, and cytochrome P4501A induction in pink salmon larvae

continuously exposed to oil-contaminated gravel during development. Can. J. Zool. 75, 989–1007.
Matsunawa, M., Akagi, D., Uno, S., Endo-Umeda, K., Yamada, S., Ikeda, K., Makishima, M., 2012. Vitamin D receptor activation enhances benzo[a]pyrene metabolism via CYP1A1 expression in macrophages. Drug Metab. Dispos. 40, 2059–2066.
McDonnell, D.P., Scott, R.A., Kerner, S.A., O'Malley, B.W., Pike, J.W., 1989. Functional domains of the human vitamin D3 receptor regulate osteocalcin gene expression. Mol. Endocrinol. 3, 635–644.
Mizwicki, M.T., Keidel, D., Bula, C.M., Bishop, J.E., Zanello, L.P., Wurtz, J.M., Moras, D., Norman, A.W., 2004. Identification of an alternative ligand-binding pocket in the nuclear vitamin D receptor and its functional importance in 1alpha,25(OH)2-vitamin D3 signaling. Proc. Natl. Acad. Sci. U. S. A. 101, 12876–12881.
Moras, D., Gronemeyer, H., 1998. The nuclear receptor ligand-binding domain: structure and function. Curr. Opin. Cell Biol. 10, 384–391.
Ngan, C.-H., Beglov, D., Rudnitskaya, A.N., Kozakov, D., Waxman, D.J., Vajda, S., 2009. The structural basis of pregnane X Receptor binding promiscuity. Biochemistry 48, 11572–11581.
Nishikawa, J.-i., Kitaura, M., Matsumoto, M., Imagawa, M., Nishihara, T., 1994. Difference and similarity of DNA sequence recognized by VDR homodimer and VDR/RXR heterodimer. Nucleic Acids Res. 22, 2902–2907.
Notredame, C., Higgins, D.G., Heringa, J., Thornton., J., 2000. T-coffee: a novel method for fast and accurate multiple sequence alignment11Edited by. J. Mol. Biol. 302, 205–217.
Nurminen, V., Seuter, S., Carlberg, C., 2019. Primary Vitamin D target genes of human monocytes. Frontiers in Physiology 10, 194.
Olsvik, P.A., Softeland, L., Lie, K.K., 2008. Selection of reference genes for qRT-PCR examination of wild populations of Atlantic cod Gadus morhua. BMC Res Notes 1, 47.
Otero, R., Seoane, S., Sigueiro, R., Belorusova, A.Y., Maestro, M.A., Perez-Fernandez, R., Rochel, N., Mourino, A., 2016. Carborane-based design of a potent vitamin D receptor agonist. Chem. Sci. 7, 1033–1037.
Pampanin, D.M., Sydnes, M.O., 2013. Polycyclic aromatic hydrocarbons a constituent of petroleum: presence and influence in the aquatic environment. Hydrocarbon.
Pawlak, M., Lefebvre, P., Staels, B., 2012. General molecular biology and architecture of nuclear receptors. Curr. Top. Med. Chem. 12, 486–504.
Peleg, S., Nguyen, C.V., 2010. The importance of nuclear import in protection of the vitamin D receptor from polyubiquitination and proteasome-mediated degradation. J. Cell. Biochem. 110, 926–934.
Peng, X., Shang, G., Wang, W., Chen, X., Lou, Q., Zhai, G., Li, D., Du, Z., Ye, Y., Jin, X., He, J., Zhang, Y., Yin, Z., 2017. Fatty acid oxidation in zebrafish adipose tissue is promoted by 1α,25(OH)2D3. Cell Rep. 19, 1444–1455.
Pérez-Albaladejo, E., Rizzi, J., Fernandes, D., Lille-Langøy, R., Karlsen, O.A., Goksøyr, A., Oros, A., Spagnoli, F., Porte, C., 2016. Assessment of the environmental quality of coastal sediments by using a combination of in vitro bioassays. Mar. Pollut. Bull. 108, 53–61.
Pike, J.W., 1991. Vitamin D3 receptors: structure and function in transcription. Annu. Rev. Nutr. 11, 189–216.
Pike, J.W., Meyer, M.B., 2010. The Vitamin D receptor: new paradigms for the regulation of gene expression by 1,25-Dihydroxyvitamin D(3). Endocrinol. Metab. Clin. North Am. 39, 255–269.
Prosser, D.E., Jones, G., 2004. Enzymes involved in the activation and inactivation of vitamin D. Trends Biochem. Sci. 29, 664–673.
Quiroga, R., Villarreal, M.A., 2016. Vinardo: a scoring function based on Autodock Vina improves scoring, docking, and virtual screening. PLoS One 11, e0155183.
Rastinejad, F., Perlmann, T., Evans, R.M., Sigler, P.B., 1995. Structural determinants of nuclear receptor assembly on DNA direct repeats. Nature 375, 203–211.
Reschly, E.J., Krasowski, M.D., 2006. Evolution and function of the NR1I Nuclear Hormone Receptor Subfamily (VDR, PXR, and CAR) with respect to metabolism of xenobiotics and endogenous compounds. Curr. Drug Metab. 7, 349–365.
Ronquist, F., Huelsenbeck, J.P., 2003. MrBayes 3: Bayesian phylogenetic inference under mixed models. Bioinformatics 19, 1572–1574.
Sakkiah, S., Kusko, R., Pan, B., Guo, W., Ge, W., Tong, W., Hong, H., 2018. Structural changes due to antagonist binding in ligand binding pocket of androgen receptor elucidated through molecular dynamics simulations. Front Pharmacol 9, 492. https://doi.org/10.3389/fphar.2018.00492.
Schrödinger, L. 2015. The PyMOL Molecular Graphics System, Version 2.0.
Sestak, M. C., Pinette, J. A., Lamoureux, C. M. & Whittemore, S. L. 2018. Early Exposure to Polycyclic Aromatic Hydrocarbons (PAHs) and Cardiac Toxicity in a Species (Xenopus laevis) with Low Aryl Hydrocarbon Receptor (AHR) Responsiveness.
Stothard, P., 2000. The sequence manipulation suite: JavaScript programs for analyzing and formatting protein and DNA sequences. BioTechniques 28, 1102–1104.
Sundell, K., Bishop, J.E., Björnsson, B.T., Norman, A.W., 1992. 1,25-Dihydroxyvitamin D3 in the Atlantic cod: plasma levels, a plasma binding component, and organ distribution of a high affinity receptor. Endocrinology 131, 2279–2286.
Sutton, A.L.M., MacDonald, -.P.N., 2003. Vitamin D: more than a "bone-a-fide" hormone. Mol. Endocrinol.
Suzuki, T., Suzuki, N., Srivastava, A.S., Kurokawa, T., 2000. Identification of cDNAs encoding two subtypes of vitamin D receptor in flounder, Paralichthys olivaceus. Biochem. Biophys. Res. Commun. 270, 40–45.
Sørensen, L., Sørhus, E., Nordtug, T., Incardona, J.P., Linbo, T.L., Giovanetti, L., Karlsen, Ø., Meier, S., 2017. Oil droplet fouling and differential toxicokinetics of polycyclic aromatic hydrocarbons in embryos of Atlantic haddock and cod. PLoS One 12 e0180048-e0180048.
Sørhus, E., Edvardsen, R.B., Karlsen, Ø., Nordtug, T., van der Meeren, T., Thorsen, A., Harman, C., Jentoft, S., Meier, S., 2015. Unexpected interaction with dispersed crude oil droplets drives severe toxicity in Atlantic haddock embryos. PLoS One 10 e0124376-e0124376.
Sørhus, E., Incardona, J.P., Karlsen, Ø., Linbo, T., Sørensen, L., Nordtug, T., van der Meeren, T., Thorsen, A., Thorbjørnsen, M., Jentoft, S., Edvardsen, R.B., Meier, S., 2016. Crude oil exposures reveal roles for intracellular calcium cycling in haddock craniofacial and cardiac development. Sci. Rep. 6, 31058.
Taketani, Y., Segawa, H., Chikamori, M., Morita, K., Tanaka, K., Kido, S., Yamamoto, H., Iemori, Y., Tatsumi, S., Tsugawa, N., Okano, T., Kobayashi, T., Miyamoto, K.-i., Takeda, E., 1998. Regulation of Type II Renal Na+-dependent Inorganic Phosphate Transporters by 1,25-Dihydroxyvitamin D3. J. Biol. Chem. 273, 14575–14581.
Takeuchi, A., Okano, T., Kobayashi, T., 1991. The existence of 25-hydroxyvitamin D3-1α-hydroxylase in the liver of carp and bastard halibut. Life Sci. 48, 275–282.
Tørresen, O.K., Star, B., Jentoft, S., Reinar, W.B., Grove, H., Miller, J.R., Walenz, B.P., Knight, J., Ekholm, J.M., Peluso, P., Edvardsen, R.B., Tooming-Klunderud, A., Skage, M., Lien, S., Jakobsen, K.S., Nederbragt, A.J., 2017. An improved genome assembly uncovers prolific tandem repeats in Atlantic cod. BMC Genomics 18, 95.
Umesono, K., Evans, R.M., 1989. Determinants of target gene specificity for steroid/thyroid hormone receptors. Cell 57, 1139–1146.
Vandesompele, J., Preter, K.D., Pattyn, F., Poppe, B., Roy, N.V., Paepe, A.D., Speleman, F., 2002. Accurate normalization of real-time quantitative RT-PCR data by geometric averaging of multiple internal control genes. Genome Biol. 3.
Velazquez-Libera, J.L., Duran-Verdugo, F., Valdes-Jimenez, A., Nunez-Vivanco, G., Caballero, J., 2020. LigRMSD: a web server for automatic structure matching and RMSD calculations among identical and similar compounds in protein-ligand docking. Bioinformatics 36, 2912–2914.
Vethaak, A.D., Davies, I.M., Thain, J.E., Gubbins, M.J., Martínez-Gómez, C., Robinson, C. D., Moffat, C.F., Burgeot, T., Maes, T., Wosniok, W., Giltrap, M., Lang, T., Hylland, K., 2017. Integrated indicator framework and methodology for monitoring and assessment of hazardous substances and their effects in the marine environment. Mar. Environ. Res. 124, 11–20.
Vikebø, F.B., Rønningen, P., Lien, V.S., Meier, S., Reed, M., Ådlandsvik, B., Kristiansen, T., 2014. Spatio-temporal overlap of oil spills and early life stages of fish. ICES J. Mar. Sci. 71, 970–981. https://doi.org/10.1093/icesjms/fst131.
Väisänen, S., Ryhänen, S., Saarela, J.T.A., Peräkylä, M., Andersin, T., Mäenpää, P.H., 2002. Structurally and functionally important amino acids of the agonistic conformation of the human Vitamin D Receptor. Mol. Pharmacol. 62, 788.
Webb, B., Sali, A., 2014. Comparative Protein Structure Modeling Using MODELLER. Curr Protoc Bioinformatics 47, 5 6 1-5 6 32.
Westin, S., Kurokawa, R., Nolte, R.T., Wisely, G.B., McInerney, E.M., Rose, D.W., Milburn, M.V., Rosenfeld, M.G., Glass, C.K., 1998. Interactions controlling the assembly of nuclear-receptor heterodimers and co-activators. Nature 395, 199–202.
Zittermann, A., 2003. Vitamin D in preventive medicine: are we ignoring the evidence? Br. J. Nutr. 89, 552–572.